Am J Transl Res 2021;13(11):12302-12317
www.ajtr.org /ISSN:1943-8141/AJTR0134207

Original Article

The epigenetic silencing of microRNA-433 facilitates the malignant phenotypes of non-small cell lung cancer by targeting CREB1

Weige Wang[1], Chao Feng[1], Wenqiang Zhang[1], Yong Long[1], Xian'en Fa[2]

Departments of [1]Thoracic Surgery, [2]Cardiac Surgery, The Second Affiliated Hospital of Zhengzhou University, Zhengzhou 450014, He'nan Province, China

Received April 13, 2021; Accepted August 30, 2021; Epub November 15, 2021; Published November 30, 2021

Abstract: Objective: MicroRNAs (miRNAs) play a big role in the regulation of non-small cell lung cancer (NSCLC) development. The objective of this study is to determine how DNA methylation regulates miR-433 in NSCLC. Methods: The degree of DNA methylation was determined, and the relevance of miR-433 and the features of NSCLC patients were assessed. The MiR-433 and CREB1 expressions were tested, and the biological characteristics of the NSCLC cells were determined. Subcutaneous tumorigenesis in nude mice and luciferase activity assays were performed. Results: MiR-433 was downregulated, and CREB1 was upregulated in the NSCLC tissues, and the methylating rate of the C-phosphate-G (CpG) island in the miR-433 promoter region was enhanced. MiR-433 was also downregulated, and CREB1 was upregulated in the NSCLC cells and there was a low degree of promoter methylation of miR-433 in the NSCLC cells after demethylation. Upregulated miR-433 or downregulated CREB1 repressed the cell vitality and colony formation abilities and increased the amount of apoptotic A549 cells. Moreover, upregulated miR-433 also decelerated tumor growth. Conversely, the H460 cells and xenografts with reduced miR-433 or overexpressed CREB1 had contrary results. CREB1 was found to be targeted by miR-433, as verified by a luciferase activity assay. Conclusion: We found that DNA methylation can downregulate miR-433 in NSCLC, which promotes the malignant behaviors of NSCLC cells.

Keywords: DNA methylation, microRNA-433, non-small cell lung cancer, cyclic-AMP responsive element binding protein 1, C-phosphate-G island, promoter region

Introduction

Lung cancer is the most familiar human malignancy [1, 2]. 80% of all lung cancers are NSCLC [3]. The major causes of lung cancer deaths around the world are pollution, smoking, and unhealthy toxic environments [4]. Great progress has been made in lung cancer, such as minimally invasive techniques for its treatment and diagnosis, screening, and the progress of radiation therapy (RT), including stereotactic ablation RT, immunotherapy, and targeted therapies [5]. However, the survival rate of NSCLC patients has not been significantly improved over the past 30 years [6]. Therefore, there is an imperative need to explore therapeutic strategies for lung cancer.

MicroRNAs (miRNAs) are small non-coding molecules with a length of 19-24 nucleotides, and miRNAs may be a critical factor in regulating the metastasis and invasion of tumor cells in all sorts of human cancers, including NSCLC [7]. It has been found that miR-1285-5p can affect the biological processes of NSCLC cells [8]. Another study has clarified that miR-204 restrains the invasion and migration of NSCLC via targeting Janus kinase 2 [9]. Also, the metastasis and proliferation of colorectal cancer are regulated by cyclic adenosine monophosphate (cAMP) responsive element binding protein 1 (CREB1)/miR-433 reciprocal feedback loop [10]. It is thought that MiR−433 suppresses NSCLC cell growth by directly targeting E2F transcription factor 3 [11]. A study has demonstrated the effect of acquired CREB1 activity impairment on cisplatin resistance in patients with metastatic NSCLC [12]. CREB1, situated at human chromosome 2q34 with a length of 75.7 kb, participates in the cAMP sig-

naling pathway [13]. According to Janica et al., the cyclic GMP/protein kinase G type-Iα signaling pathway advances CREB phosphorylation, maintains the high expression of c-IAP1, and inhibits the synergistic effect of PKG-Iα kinase activity with cisplatin in NSCLC [14]. Moreover, the P21-activated kinase 1/CREB axis has been found to be elevated in squamous NSCLC [15]. DNA methylation data indicate the impact of external factors on patients and is thought to be a new star in cancer research. DNA methylation data can be utilized for gene screening, serving as pivotal roles in cancer development, progress and metastasis [16]. It has been shown that the C-phosphate-G (CpG) islands around miR-433 are hypermethylated [17]. In this research, we therefore examined the expressions and function of DNA methylated miR-433 in NSCLC with the involvement of CREB1.

Materials and methods

Study subjects

From 2011 to 2013, 94 stage I NSCLC patients (63 males and 31 females; aged 32-76 years; median age of 63 years) treated in the thoracic surgery department in our hospital were recruited as the study cohort. The tumor-node-metastasis (TNM) stage of patients included 59 cases of stages I/II and 35 cases of stages III/IV. The cases were histologically classified as 25 cases of adenosquamous carcinoma, 39 cases of adenocarcinoma and 30 cases of squamous cell carcinoma.

Inclusion criteria: patients with complete follow-up data and postoperative pathological specimens; patients who underwent radical surgical treatment; and patients who didn't undergo radiotherapy, chemotherapy, or biotherapy before or after their operations; and patients who didn't die during the operation or who died from non-tumor causes after their operations.

The normal epithelial tissues of the lungs 3-5 cm from the edge of lung cancer tissues were set as the controls for the NSCLC tissues. All the tissue samples were cut into small pieces and quickly stored in liquid nitrogen in a frozen tube, and then moved to a freezer at -80°C. Our study was approved by the ethics committee of our university, and the approval number was 2016-089. All the patients provided a written informed consent.

Cell selection and culture

16HBE, A549, H1299, PGCL3, SK-MES-1 and H460 cells were bought from the American Type Culture Collection (Rockefeller, Maryland, USA). The A549, H1299, PGCL3, SK-MES-1 and 16HBE cell lines were incubated in a DMEM containing 10% FBS, and the H460 cell line was incubated in RPMI 1640 medium containing 10% FBS (Gibco, Grand Island, NY, USA) in a 5% CO_2 incubator. The MiR-433 and CREB1 expressions in the cell lines was measured using RT-qPCR. The cell lines with the largest and smallest different expressions of miR-433 and CREB1 were used for the subsequent cell experiments.

Demethylation

The A549 and H460 cells were incubated in a DMEM or RPMI 1640 medium containing 10% FBS and treated with 10 μM 1% 5-azacytidine (5-Aza) (Sigma, St. Louis, MO, USA) then dissolved using dimethyl sulfoxide (DMSO) for 72 h to obtain the A549 5-Aza group and the H460 5-Aza group. The cells were treated with the same amount of DMSO to obtain the A549 control group and the H460 control group to test the methylation of the cells.

Methylation-specific PCR (MSP)

The genomic DNA was abstracted and transformed using EpiTect fast DNA Bisulfite kits (Shanghai Limin Industrial Co., Ltd., Shanghai, China). The cDNA was purified and retrieved using reagent kits with self-contained centrifugal columns, and stored at -20°C for use. The methylation levels of the miR-433 promoter region were verified using EpiTect MSP kits (Univ Biotechnology Co., Ltd., Shanghai, China) specification. The primer sequences are shown in **Table 1**. Electrophoresis was utilized for the amplification product, and ultraviolet light was irradiated for the banding. Methylation rate = amount of methylated positive specimens/total number of specimens ×100%.

Cell grouping

A549 cells were distributed into 7 groups and respectively treated with an miR-433 mimic, siRNA-CREB1, Oe-CREB1 or the negative control (NC). Among them, the mimic-NC, the miR-433 mimic, siRNA-NC, and siRNA-CREB1 were composed by GenePharma Ltd Company (Shanghai, China). The sequences of

Table 1. The methylation primer sequences

Gene	Sequence (5'→3')
Methylated miR-433	F: 5'-TTTGGGTTGGGATGGTGTTTG-3'
	R: 5'-ACACCCTAACCCTAAACAACCATCC-3'
Unmethylated miR-433	F: 5'-GGGCCCCTCTTCATGCCACTCGG-3'
	R: 5'-AGGTGCCCATCATGATCCTTCTCAAC-3'

Note: F: forward; R: reverse; miR-433: microRNA-433.

Table 2. The transfection sequences

	Sequence (5'→3')
miR-433 mimic	5'-AUCAUGAUGGGCUCCUCGGUGU-3'
miR-NC	5'-UUCUCCGAACGUGUCACGUTT-3'
siRNA-CREB1	5'-GCAGCUCGAGAGUGUCGUATT-3'
siRNA-NC	5'-UUCUCCGAACGUGUCACGUTT-3'

Note: miR-433: microRNA-433; CREB1: cyclic-AMP responsive element binding protein 1.

Table 3. The primer sequences

Gene	Sequence (5'→3')
miR-433	F: 5'-GGATCATGATGGGCTCCT-3'
	R: 5'-CAGTGCGTGTCGTGGAGT-3'
U6	F: 5'-GCTTCGGCAGCACATATACTAAAAT-3'
	R: 5'-CGCTTCACGAATTTGCGTGTCAT-3'
CREB1	F: 5'-AGACTTCAGCACCTGCCATC-3'
	R: 5'-TGTCCATCAGTGGTCTGTGC-3'
GAPDH	F: 5'-CGGAGTCAACGGATTTGGTCGTAT-3'
	R: 5'-AGCCTTCTCCATGGTGGTGAAGAC-3'

Note: F: forward; R; reverse; miR-433: microRNA-433; CREB1: cyclic-AMP responsive element binding protein 1; GAPDH: glyceraldehyde phosphate dehydrogenase.

miR-433 mimic, miR-NC, siRNA-CREB1, and siRNA-NC are listed in **Table 2**. Oe-CREB1 was formed by cloning the CREB1 full-length sequence into a pcDNA3.1 vector (Shanghai Sangon Biotechnology Co., Ltd., Shanghai, China), while the Oe-NC was the pcDNA3.1 vector (the empty vector). H460 cells were distributed into the 7 groups and treated with the miR-433 inhibitor, Oe-CREB1, siRNA-CREB1, or the NC. Among them, inhibitor-NC, miR-433 inhibitor and siRNA-CREB1 were composed by GenePharma, and the Oe-NC and Oe-CREB1 were bought from Sangon Biotechnology. The cells were cultured into a 12-well plate for 24 h, and 1.5 mL penicillin-streptomycin-free full culture solution was appended to each well. When the confluence reached about 60% during infection, the A549 and H460 cells were transiently transfected with lipofectamine 2000, and the fluid was renewed after 6-h transfection. The cells were harvested for the subsequent experiments 48 h post incubation.

RT-qPCR

According to the manufacturer's protocol, TRIzol reagent (Invitrogen) was used to extract the total RNA. The cDNA was gained using AMV reverse transcription (NEB, USA) of 1 μg RNA. The SYBR Green (Premix ExTaq™ kit, Takara Biotech, Dalian, China) method was utilized to carry out qPCR. The reactions were performed at 95°C for 10 min followed by 40 cycles at 95°C for 15 sec of denaturation, at 60°C for 1 min of annealing, and at 72°C for 20 sec of extension. The PCR primers are shown in **Table 3**. U6 and GAPDH were used as internal parameters. The product was validated using agarose gel electrophoresis. The data were measured using $2^{-\Delta\Delta Ct}$.

Western blot analysis

The proteins were abstracted, and the concentration was measured using bicinchoninic acid kits (Wuhan Boster Biological Technology Co., Ltd., Hubei, China). Polyacrylamide gel (10%, Boster Biological Technology) was used to separate the protein. The protein was transferred to PVDF membranes and blocked with 5% nonfat milk powder for 1 h. Next, the primary antibodies against CREB1 (1:500) and GAPDH (1:3000, Abcam, MA, USA) were incubated overnight at 4°C. The corresponding secondary antibody (ZSGB-Bio, Beijing, China) was incubated for 1 h. The membrane was cleaned 3 times/5 min. The chemiluminescence reagent and Gel Doc EZ Imager (Bio-Rad, California, USA) were utilized and explicated using Image J software.

CCK-8 assay

The cell suspension was seeded into a 96-well plate at a density of 1×10^3 cells/100 μL/well after the cells were diluted, and five parallel wells were set. Five duplicates were set at each time point according to the culture for 7 d. The CCK-8 solution (10 μL, Sigma) was added and incubated for 4 h. The OD values were tested at 450 nm.

Colony formation assay

The cells were trypsinized, and the cell suspension was fully dispersed. The cells (200) were

seeded into 6-well plates and cultured for 2-3 weeks. When the cell colony was visible to the naked eye, the culture was terminated and the cells were fixed with 4% paraformaldehyde. Then cells were dyed with Giemsa solution for 60 min.

Flow cytometry

Cell cycle analysis: The cells were harvested by centrifugation and mixed with about 70% cold ethanol (500 μL) and fixed overnight at 4°C for 2 h. The stationary solution was further eluted by 1 mL phosphate buffer saline (PBS), and the cells were centrifuged at 2000 rpm for 3 min. The cells were rinsed with 100 μL RNase A (Solarbio, Beijing, China) at 37°C for 30 min, then mixed with 400 μL propidium iodide (PI, Sigma-Aldrich, USA) staining and verified using a flow cytometry (BD Biosciences, Franklin Lakes, NJ, USA) after avoiding light for 30 min at 4°C. The red fluorescence at 488 nm was recorded.

Cell apoptosis assay: The cells (1×10^6 cells/mL, 200 μL) were centrifuged. The cells were re-suspended in 100 μL binding buffer, appended with Annexin-V-FITC (Beijing Biosea Biotechnology, Beijing, China) for 15 min, then mixed with 300 μL PBS and mixed with PI solution before being placed on the flow cytometer, and the analysis was carried out on the flow cytometer within 30 min. The cell apoptosis was determined as previously described [18].

Transwell assay

Cells were seeded on the Transwell chamber and incubated for 24 h. Then the unmigrated cells were removed, and the cells were fixed with formaldehyde for 30 min. After fixation, the cells were dyed with 0.5% crystal violet solution for 20 min. Five visual fields were randomly selected to count the migrated cells, and pictures were taken using an inverted microscope. The chamber in the cell invasion test was coated with 50 μL Matrigel solution in advance.

Subcutaneous tumorigenesis in the nude mice

Thirty adult BALB/c-nude mice (Vital River Laboratory Animal Technology Co., Ltd., Beijing, China) were fed under a specific pathogen-free environment in the animal center with free access to sterile food and water.

Well-grown A549 and H460 cells were adjusted to 4×10^6 cells/0.1 mL PBS. Each mouse was injected with 4 wer^6 cells in their backs (n = 5), and then they were observed every 5 d. The tumor sizes and mouse weights were measured. Tumor volume = (π/6) π/L π/l^2 (L: length diameter; l: width diameter). Thirty days after injection, the mice were euthanized using CO_2 and the xenografts were isolated, photographed, and weighed.

Dual luciferase reporter gene assay

3'UTR of CREB1 was cloned and amplified into the luciferase vector of pmirGLO, as CREB-wild type (WT). A CREB1-mutant type (MUT) vector was constructed respectively, with the pRL-TK vector (E2241, Promega) expressing renilla luciferase as the internal reference. The MiR-433 mimic and the miR-433 mimic NC were separately co-transfected with the luciferase reporter vector into A549 and H460 cells.

Statistical analysis

All the data were processed using SPSS 21.0 software (IBM Corp. Armonk, NY, USA). The measurement data are shown as the means ± standard deviations. t-tests were conducted for the two-group comparisons and ANOVA was used for the multiple-group comparisons, and Fisher's LSD-t tests were utilized after ANOVA. The relationship between miR-133a and the clinical features of NSCLC were evaluated using chi-square tests. $P<0.05$ was considered significantly different.

Results

The MiR-433 expressions were downregulated and CREB1 was upregulated in the NSCLC tissues, and the methylating rate of the CpG island was raised in the miR-433 promoter region

In contrast with the corresponding adjacent normal tissues, the miR-433 expressions were decreased and the CREB1 expression was elevated in the NSCLC tissues ($P<0.05$) (**Figure 1A** and **1B**). Methylation-positive (complete or partial methylation) referred to the amplification of the M-band, with or without the U-band. Methylation-negative referred to the expansion of the U-band without the M-band, and neither the U nor the M-band could be amplified as a deletion of the gene copy. Case l showed miR-433 methylation-negative, while cases 2 3 were miR-433 methylation-positive (**Figure**

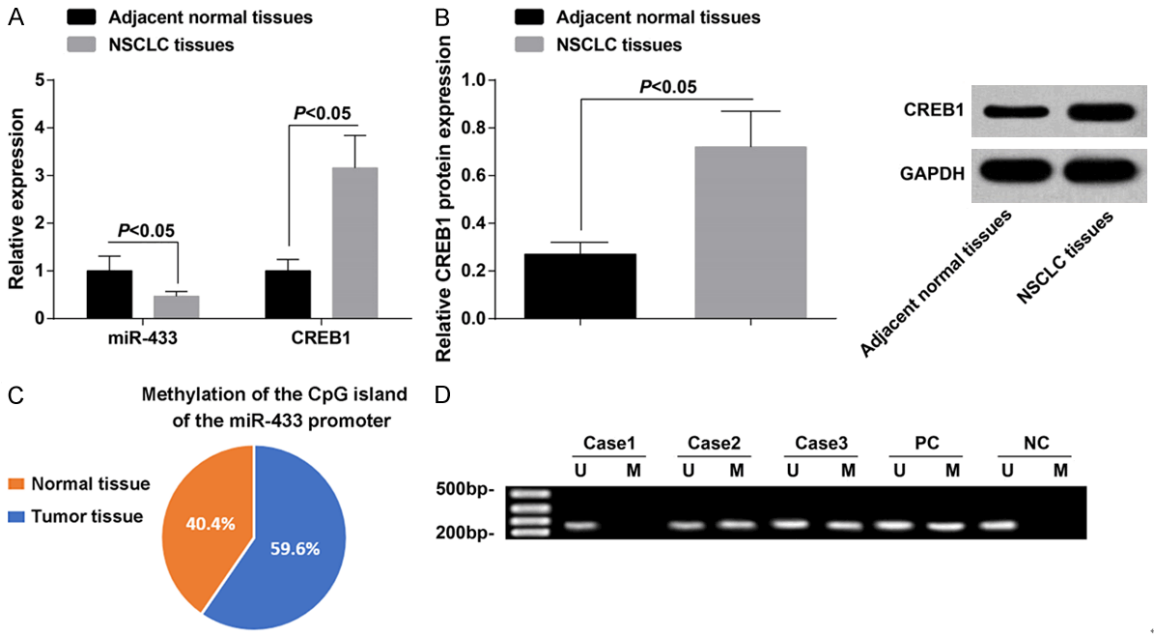

Figure 1. The miR-433 expressions are reduced and the CREB1 expressions were enhanced in the NSCLC tissues, and the methylating rate of the CpG island was raised in the miR-433 promoter region. A: Quantification of the miR-433 and CREB1 expressions in the NSCLC tissues and corresponding adjacent normal tissues using RT-qPCR; B: Quantification of the protein expressions of CREB1 in the NSCLC tissues and the corresponding adjacent normal tissues using Western blot analyses; C: The methylation rate of the CpG island of the miR-433 promoter in the NSCLC tissues (n = 94) and the adjacent normal tissues. D: The methylated status of miR-433 in the tissues measured using MSP. U, unmethylated band, M, methylated band, NC, negative control, PC, positive control; n = 94, Cases 1-3 expressed for the 3 screened representative cases. The measurement data were depicted as the mean ± standard deviation. The comparisons between two groups were conducted using *t* tests. CREB1: cyclic-AMP responsive element binding protein 1; NSCLC: non-small cell lung cancer; MSP: Methylation-specific PCR; miR-433: microRNA-433.

1D). The results indicated that the methylation rate of the CpG island of the miR-433 promoter in the NSCLC tissues was heightened versus the adjacent normal tissues (59.6% (56/94) VS 40.4% (38/94), P<0.05) (**Figure 1C**).

The miR-433 expressions are related to the TNM stages and the smoking histories of the NSCLC patients

The NSCLC patients were separated into low miR-433 and high miR-433 expression groups. The data indicated that the TNM stage and smoking histories were correlated with miR-433 (P<0.01), but age, gender, pathological type and the NSCLC differentiation degree were not related to miR-433 (P>0.05) (**Table 4**).

Low expressions of miR-433 and high expressions of CERB1 in the NSCLC cells and a low degree of promoter methylation were observed in the miR-433 in A549 and H460 cells after demethylation

The MiR-433 and CREB1 expressions in the 16HBE cells and the NSCLC cell lines were verified. It was briefly shown that, in contrast to human bronchial epithelial cell line 16HBE, the miR-433 expression was decreased and the CERB1 expression was elevated in the NSCLC cell lines (all P<0.05). Among the NSCLC cell lines, the A549 cells had the largest, and the H460 cells had the smallest difference from the 16HBE cells (**Figure 2A** and **2B**). Therefore, further experiments were conducted on the A549 cells that were treated with the miRNA-433 mimic and/or siRNA-CREB1 and H460 cells that were treated with miRNA-433 inhibitor and/or OE-CREB1 to verify the effects of miRNA-433 and CREB1 on the lung cancer cell functions.

MSP was used to determine the methylation level of the CpG island in the miR-433 promoter regions of the NSCLC cell lines, the results of which showed that the methylation level of the miR-433 promoter region in the A549 cells was the highest and in the H460 cells was the lowest (**Figure 2C**).

The A549 and H460 cells were demethylated by 5-Aza and then MSP was used to verify the

Table 4. The relationship between the relative expressions of miR-433 and the clinicopathological features in NSCLC patients

Clinicopathologic data	n	Expression of miR-433		P
		Low expression group (n = 47)	High expression group (n = 47)	
Age (years)				0.535
≤63	43	23	20	
>63	51	24	27	
Gender				0.273
Male	63	34	29	
Female	31	13	48	
TNM stage				0.019
I/II	59	24	35	
IIII/IV	35	23	12	
Pathological type				0.209
Adenosquamous carcinoma	25	14	11	
Adenocarcinoma	39	22	17	
Squamous cell carcinoma	30	11	19	
Differentiation				0.410
High	32	19	13	
Moderate	31	18	23	
Poor	21	10	11	
Smoking history				0.001
Smoking	61	38	23	
Non-smoking	33	9	24	

Note: miR-433: microRNA-433; TNM stage: tumor-node-metastasis stage; NSCLC: non-small cell lung cancer. The data in this table were enumeration data and were analyzed using chi-square tests.

promoter methylation of miR-433. Together, these data support the conclusion that the methylation degrees of the miR-433 promoter in the A549 and H460 cells were reduced, but the methylation in the H460 cells was slightly lower than it was in the A549 cells, and the miR-433 expressions in the H460 cells and A549 cells were the opposite (all P<0.05) (**Figure 2D** and **2E**).

Upregulated miR-433 or downregulated CREB1 suppressed the cell viability and colony formation abilities of the A549 cells, and downregulated miR-433 or upregulated CREB1 induced the cell viability and colony formation ability of the H460 cells

The CCK-8 assays and the colony formation assays indicated that siRNA-CREB1 or the miR-433 mimic suppressed the cell viability and the colony formation abilities in the A549 cell with low miR-433 expression but Oe-CREB1 reversed the effect of the miR-433 mimic on the cell viability and colony formation ability in the A549 cells (**Figure 3A**, **3C** and **3D**). On the contrary, the cell viability and colony formation abilities were elevated by Oe-CREB1 or the miR-433 inhibitor in the H460 cells with high miR-433 expressions, while siRNA-CREB1 abolished the effect of the miR-433 inhibitor on the cell viability and colony formation ability in the A549 cells (P<0.05) (**Figure 3B**, **3E** and **3F**).

The overexpression of miR-433 or the low expression of CREB1 increases the apoptosis in A549 cells while upregulating CREB1 or silencing miR-433 represses the apoptosis in the H460 cells

The cell cycle changes in each group after the transfection were verified using flow cytometry. As shown in **Figure 4A** and **4B**, the proportions of the G0/G1 phase cells were raised, and the proportions of the S and G2/M phase cells were depressed by the siRNA-CREB1 or the miR-433 mimic group, and the effect of the miR-433 mimic was eliminated by Oe-CREB1 in the A549 cells. Conversely, the proportions of the S and G2/M phase cells were elevated, and the proportions of the G0/G1 phase cells were depressed using the Oe-CREB1 or the miR-433 inhibitor, and the impact of the miR-433 inhibitor was abrogated by siRNA-CREB1 in the H460 cells (**Figure 4C** and **4D**).

Flow cytometry was used to evaluate the changes in the apoptosis rate in each group after the transfection. It showed that the siRNA-CREB1 or the miR-433 mimic enhanced the apoptosis rate, while Oe-CREB1 reversed the effect of the miR-433 mimic (**Figure 5A** and **5B**). On the other hand, Oe-CREB1 or the miR-

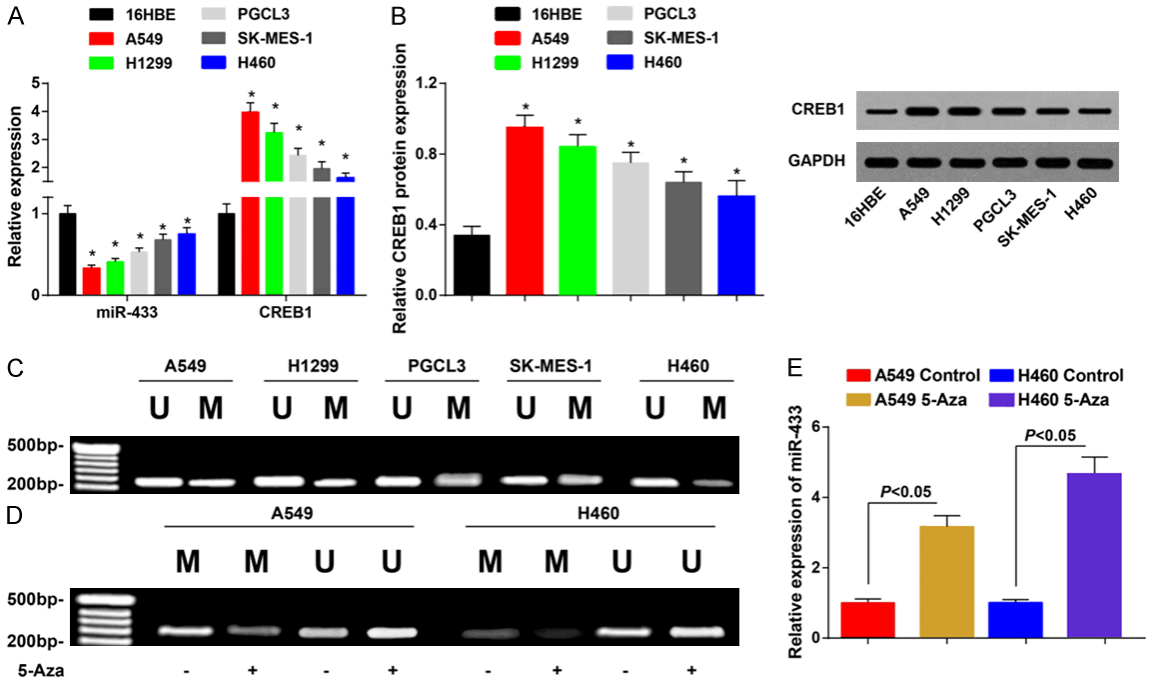

Figure 2. The downregulation of miR-433 and the upregulation of CREB1 in the NSCLC cells and the low degree of promoter methylation of miR-433 in the A549 and H460 cells after demethylation. A: The expressions of miR-433 and CREB1 in the NSCLC cells and in bronchial epithelial cell 16HBE were measured using RT-qPCR; B: The protein expressions of CREB1 in the NSCLC cells and the bronchial epithelial cell 16HBE were measured using Western blot analyses; C: MSP assays were used to measure the methylation of the CpG island in the miR-433 promoter region in NSCLC cells; D: An MSP assay was used to measure the methylated status of miR-433 in the A549 and H460 cells after demethylation by 5-Aza. E: The expressions of miR-433 in the A549 and H460 cells after demethylation using RT-qPCR. M was a methylated band and U was an unmethylated band. n = 5 for each group. *P<0.05. The measurement data are shown as the mean ± standard deviation. The comparisons between two groups were conducted using *t* tests. The comparisons among multiple groups were assessed using one-way analyses of variance followed by LSD-t tests. MSP: Methylation-specific PCR; CREB1: cyclic-AMP responsive element binding protein 1; NSCLC: non-small cell lung cancer; miR-433: microRNA-433.

433 inhibitor reduced the apoptosis rate, and the impact of the miR-433 inhibitor was reversed by siRNA-CREB1 in the H460 cells (**Figure 5C** and **5D**).

Silencing CREB1 or upregulating miR-433 inhibited the invasion of A549 cells while upregulating CREB1 or silencing miR-433 enhanced the invasion of the H460 cells

The cell invasion changes after the transfection were verified by Transwell assays. In comparison to siRNA-NC and the mimic-NC groups, the invasive abilities of the A549 cells were decreased by siRNA-CREB1 or the miR-433 mimic, while the role of the miR-433 mimic was eliminated by the Oe-CREB1 (**Figure 6A** and **6B**). Meanwhile, the invasive abilities of the H460 cells were elevated by Oe-CREB1 or the miR-433 inhibitor, and siRNA-CREB1 abolished the impact of the miR-433 inhibitor (**Figure 6C** and **6D**).

miR-433 targets CREB1

The MiR-433 and CREB1 expressions in the A549 and H460 cells were determined. Compared to the mimic-NC group, the miR-433 expressions were raised in the miR-433 mimic group (P<0.05), and the CREB1 expressions were reduced (both P<0.05). The siRNA-CREB1 didn't affect the miR-433 expression while it downregulated CREB1. By comparison with the miR-433 mimic + Oe-NC group, the CREB1 mRNA and protein expressions in the miR-433 mimic + Oe-CREB1 group were enhanced (both P<0.05) (**Figure 7A** and **7B**). In addition, the miR-433 inhibitor downregulated miR-433 and upregulated CREB1. Oe-CREB1 overexpressed CREB1 but didn't affect the miR-433 expres-

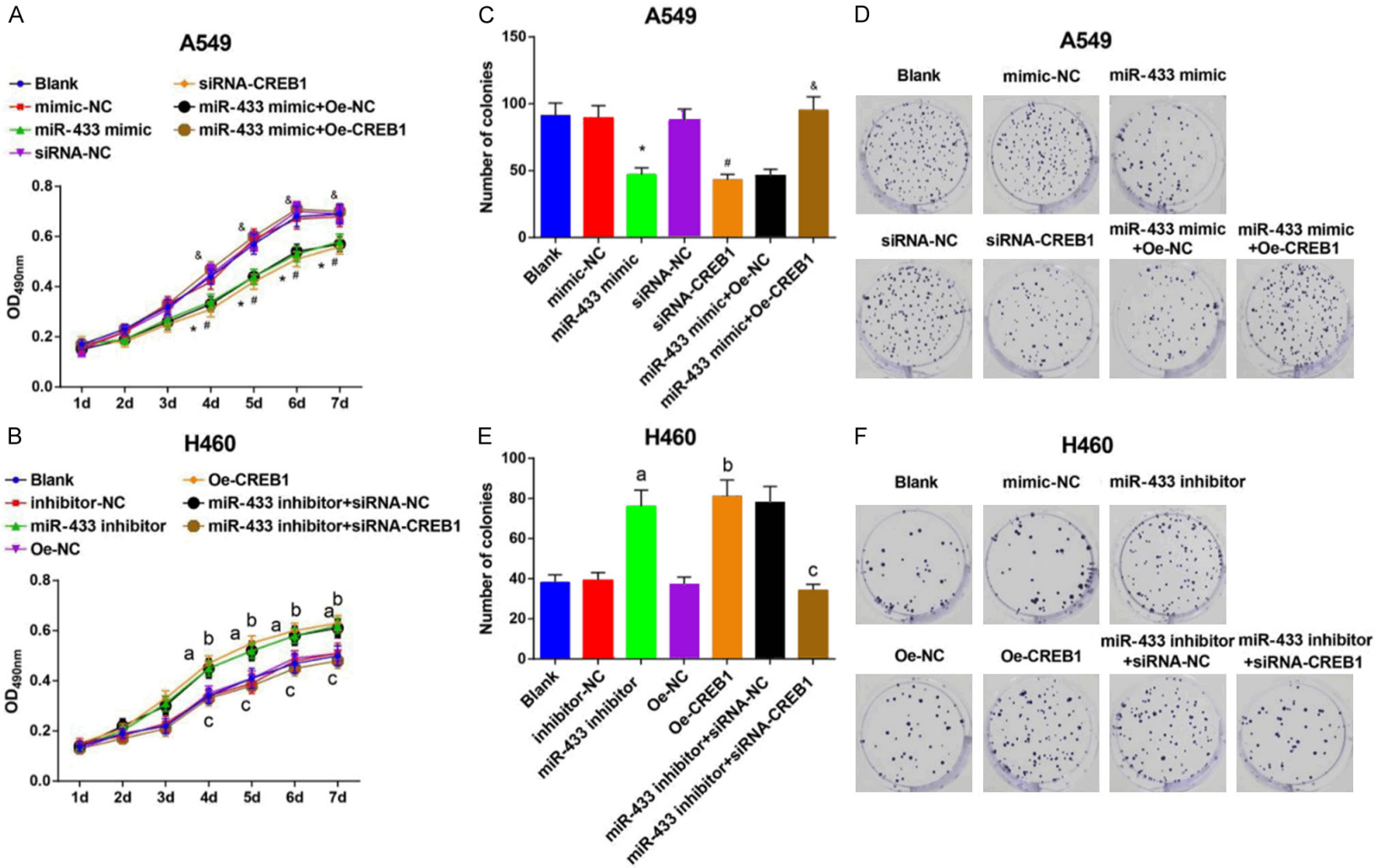

Figure 3. The upregulation of miR-433 or the downregulation of CREB1 decreases the cell viability and colony formation abilities of the A549 cells, and downregulated miR-433 or upregulated CREB1 increases the cell viability and colony formation abilities of the H460 cells. A: Measurement of the viability of the A549 cells using CCK-8 assays; B: Measurement the viability of the H460 cells using CCK-8 assays; C, D: The colony formation ability of the A549 cells in each group measured using colony formation assays; E, F: The colony formation abilities of the H460 cells in each group measured using colony formation assays. n = 5 for each group. Compared with the mimic-NC group, $^{*}P<0.05$. Compared with the siRNA-NC group, $^{\#}P<0.05$. Compared with the miR-433 mimic + Oe-NC group, $^{\&}P<0.05$. Compared with the inhibitor-NC group, $^{a}P<0.05$. Compared with the Oe-NC group, $^{b}P<0.05$. Compared with the miR-433 inhibitor + siRNA-NC group, $^{c}P<0.05$. The measurement data are depicted as the means ± standard deviations, and the comparisons among multiple groups were assessed using one-way ANOVA followed by LSD-t tests. CREB1: cyclic-AMP responsive element binding protein 1; miR-433: microRNA-433.

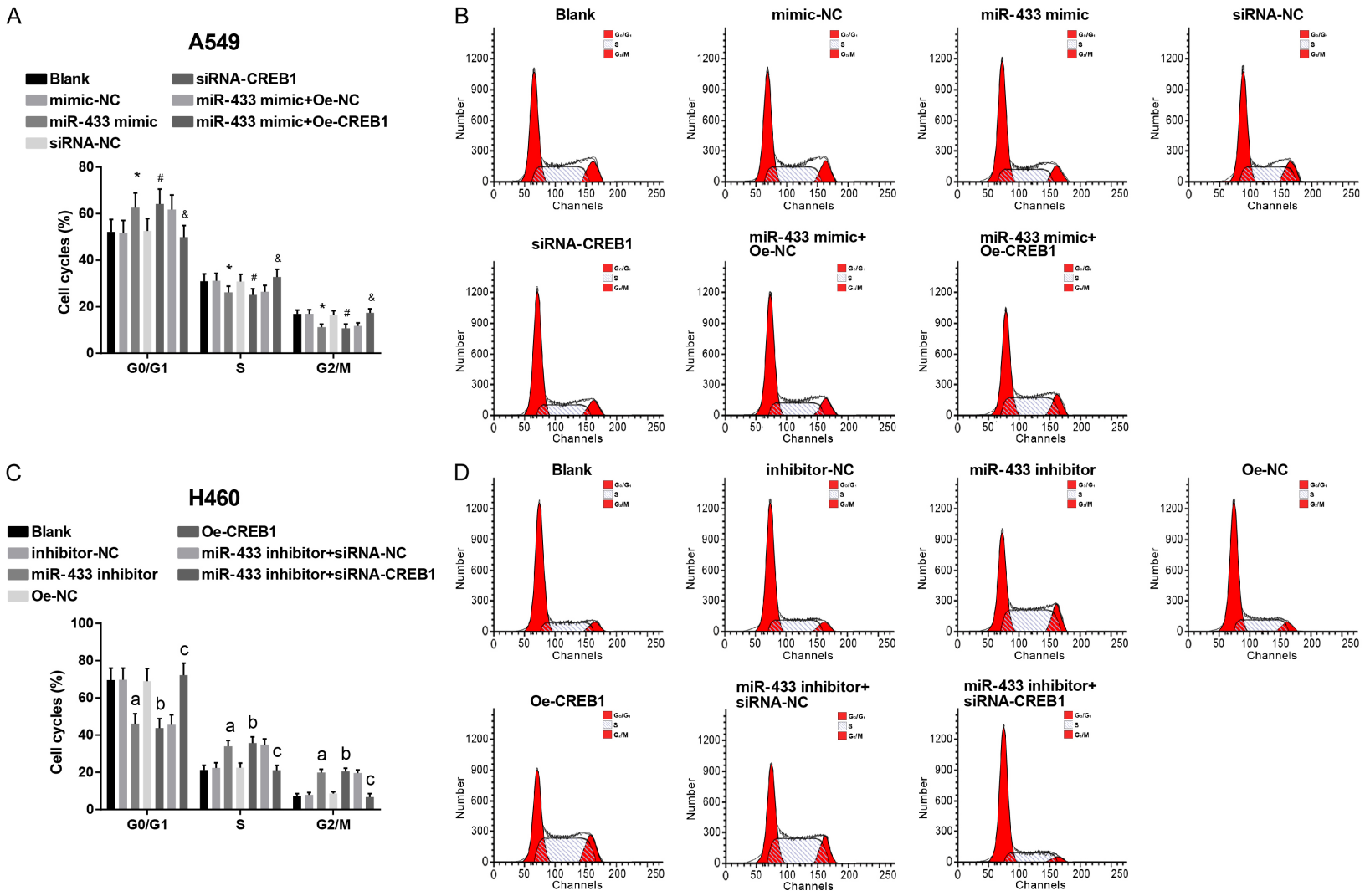

Figure 4. Upregulated miR-433 or downregulated CREB1 increases the proportion of the G0/G1 phase in A549 cells, while upregulating CREB1 or silencing miR-433 increases the proportion of the S phase in H460 cells. A, B: The cell cycle of the A549 cells in each group using flow cytometry; C, D: The cell cycle of the H460 cells in each group using flow cytometry. n = 5 for each group. Compared with the mimic-NC group, $^{*}P<0.05$. Compared with the siRNA-NC group, $^{\#}P<0.05$. Compared with the miR-433 mimic + Oe-NC group, $^{\&}P<0.05$. Compared with the inhibitor-NC group, $^{a}P<0.05$. Compared with the Oe-NC group, $^{b}P<0.05$. Compared with the miR-433 inhibitor + siRNA-NC group, $^{c}P<0.05$. The measurement data are depicted as the means ± standard deviations. The comparison among multiple groups were assessed using one-way ANOVA followed by LSD-t tests. CREB1: cyclic-AMP responsive element binding protein 1; miR-433: microRNA-433.

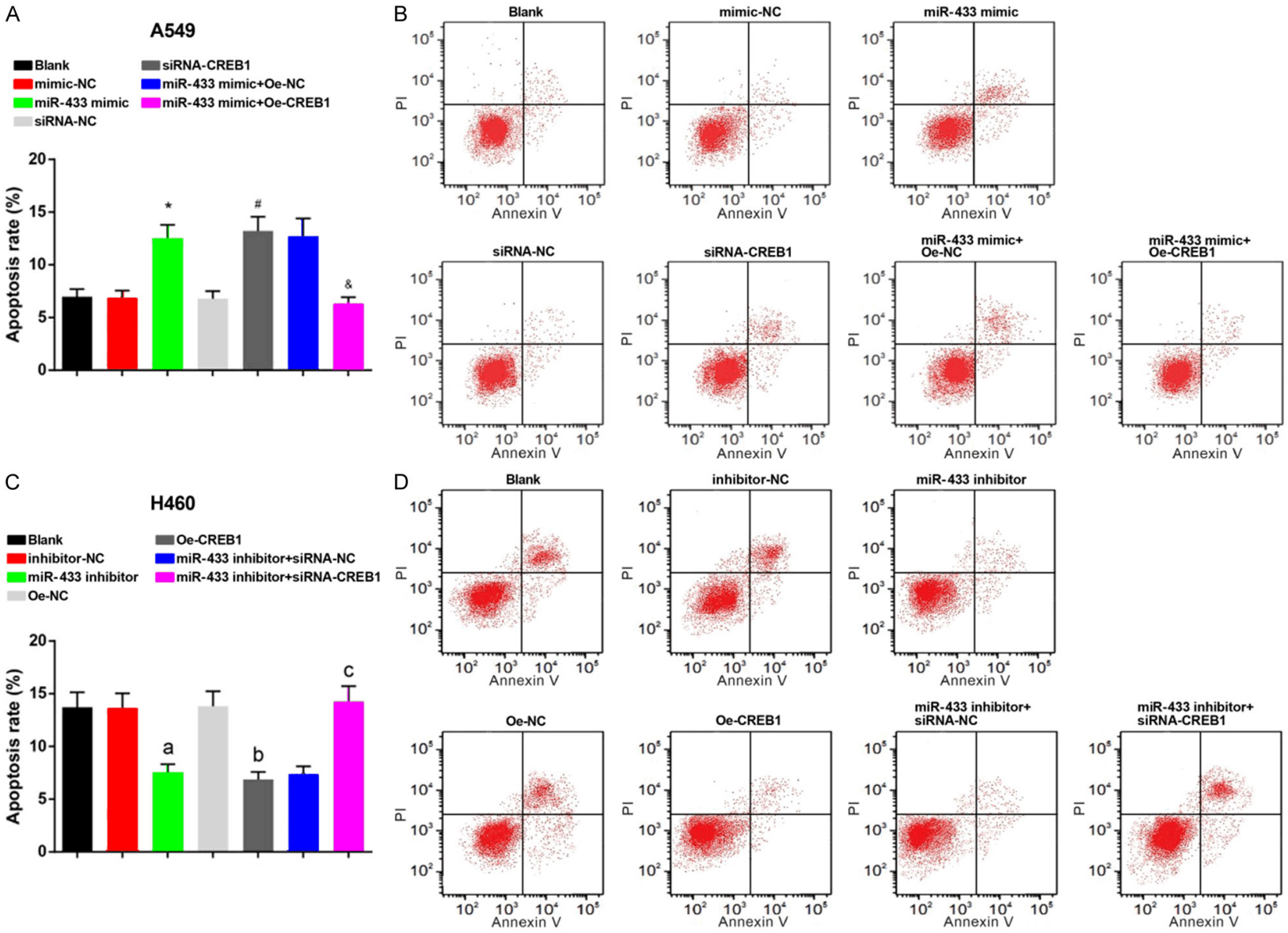
A
A549
Blank
mimic-NC
miR-433 mimic
siRNA-NC
siRNA-CREB1
miR-433 mimic+Oe-NC
miR-433 mimic+Oe-CREB1
Apoptosis rate (%)
B
Blank
mimic-NC
miR-433 mimic
siRNA-NC
siRNA-CREB1
miR-433 mimic+ Oe-NC
miR-433 mimic+ Oe-CREB1
PI
Annexin V
C
H460
Blank
inhibitor-NC
miR-433 inhibitor
Oe-NC
Oe-CREB1
miR-433 inhibitor+siRNA-NC
miR-433 inhibitor+siRNA-CREB1
Apoptosis rate (%)
D
Blank
inhibitor-NC
miR-433 inhibitor
Oe-NC
Oe-CREB1
miR-433 inhibitor+ siRNA-NC
miR-433 inhibitor+ siRNA-CREB1
PI
Annexin V

Figure 5. Upregulated miR-433 or downregulated CREB1 increases the apoptosis in A549 cells, while upregulating CREB1 or silencing miR-433 decreases apoptosis in H460 cells. A, B: Apoptosis of the A549 cells in each group using flow cytometry; C, D: Apoptosis of the H460 cells in each group using flow cytometry. n = 5 for each group. Compared with the mimic-NC group, *P<0.05. Compared with the siRNA-NC group, #P<0.05. Compared with the miR-433 mimic + Oe-NC group, &P<0.05. Compared with the inhibitor-NC group, aP<0.05. Compared with the Oe-NC group, bP<0.05. Compared with the miR-433 inhibitor + siRNA-NC group, cP<0.05. The measurement data are shown as the means ± standard deviations. The comparison among multiple groups were assessed using one-way ANOVA followed by LSD-t tests. CREB1: cyclic-AMP responsive element binding protein 1; miR-433: microRNA-433.

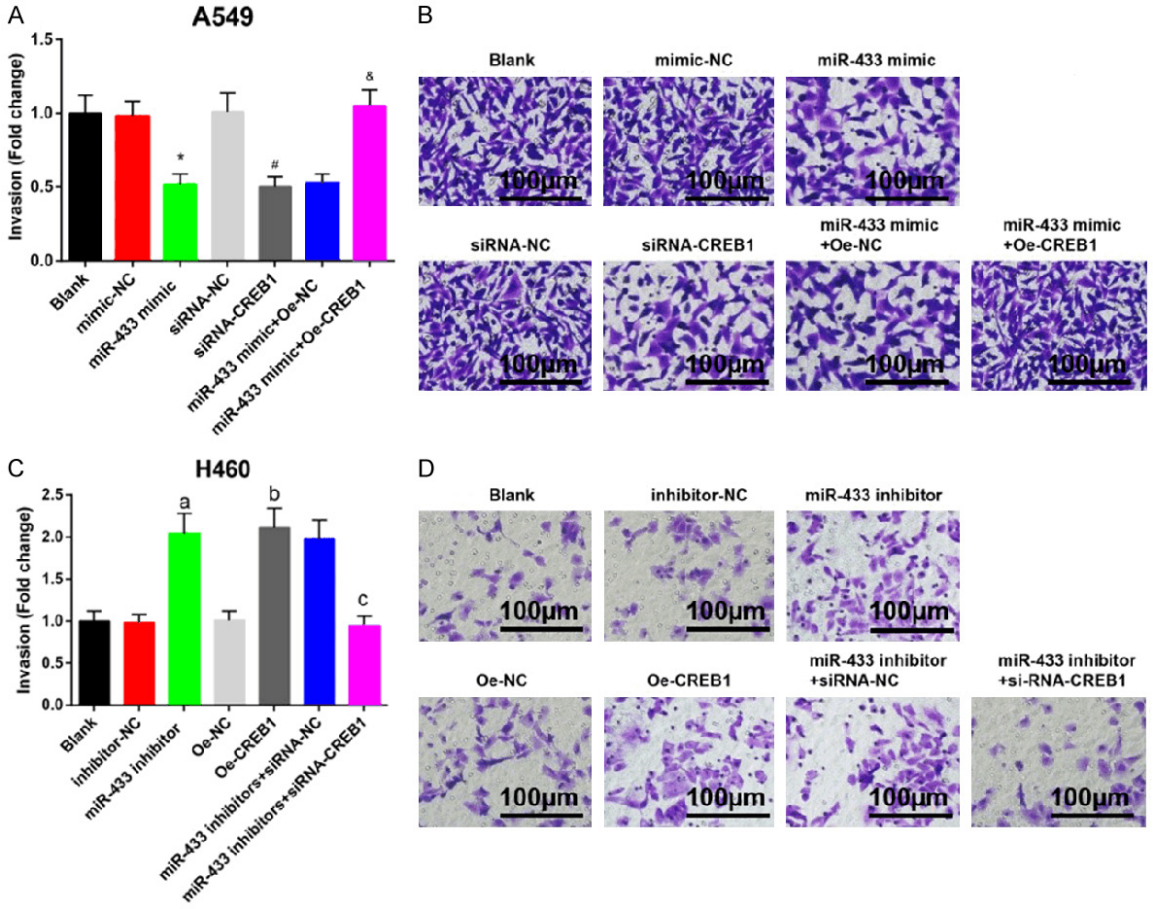

Figure 6. The upregulation of the miR-433 expression or the downregulation of the CREB1 expression decreases the invasion of A549 cells, while the overexpression of CREB1 or the downregulation of miR-433 promotes the invasion of H460 cells. A, B: The cell invasion of the A549 cells after miR-433 mimic and/or the siRNA-CREB1 treatment using Transwell assays (200×); C, D: The cell invasion of the H460 cells in each group after the miR-433 mimic and/or the siRNA-CREB1 treatment using Transwell assays. n = 5 for each group (200×). Compared with the mimic-NC group, *P<0.05. Compared with the mimic-NC group, #P<0.05. Compared with the miR-433 mimic + Oe-NC group, &P<0.05. Compared with the inhibitor-NC group, aP<0.05. Compared with the Oe-NC group, bP<0.05. Compared with the miR-433 inhibitor + siRNA-NC group, cP<0.05. Measurement data were depicted as mean ± standard deviation. The comparisons among multiple groups were assessed using one-way ANOVA followed by LSD-t tests. CREB1: cyclic-AMP responsive element binding protein 1; miR-433: microRNA-433.

sion. In contrast with the miR-433 inhibitor + siRNA-NC group, the CREB1 expression was reduced (both P<0.05) (**Figure 7C** and **7D**).

The targeted relationship between miR-433 and CREB1 was analyzed using the online software (TargetScan 4.2 (www.targetscan.org) and PicTar (http://pictar.mdcberlin.de/), and the potential binding site is shown in **Figure 7E**. The luciferase activity was restricted after the co-transfection of CREB1-WT and miR-433 mimic (P<0.05). The relative luciferase activi-

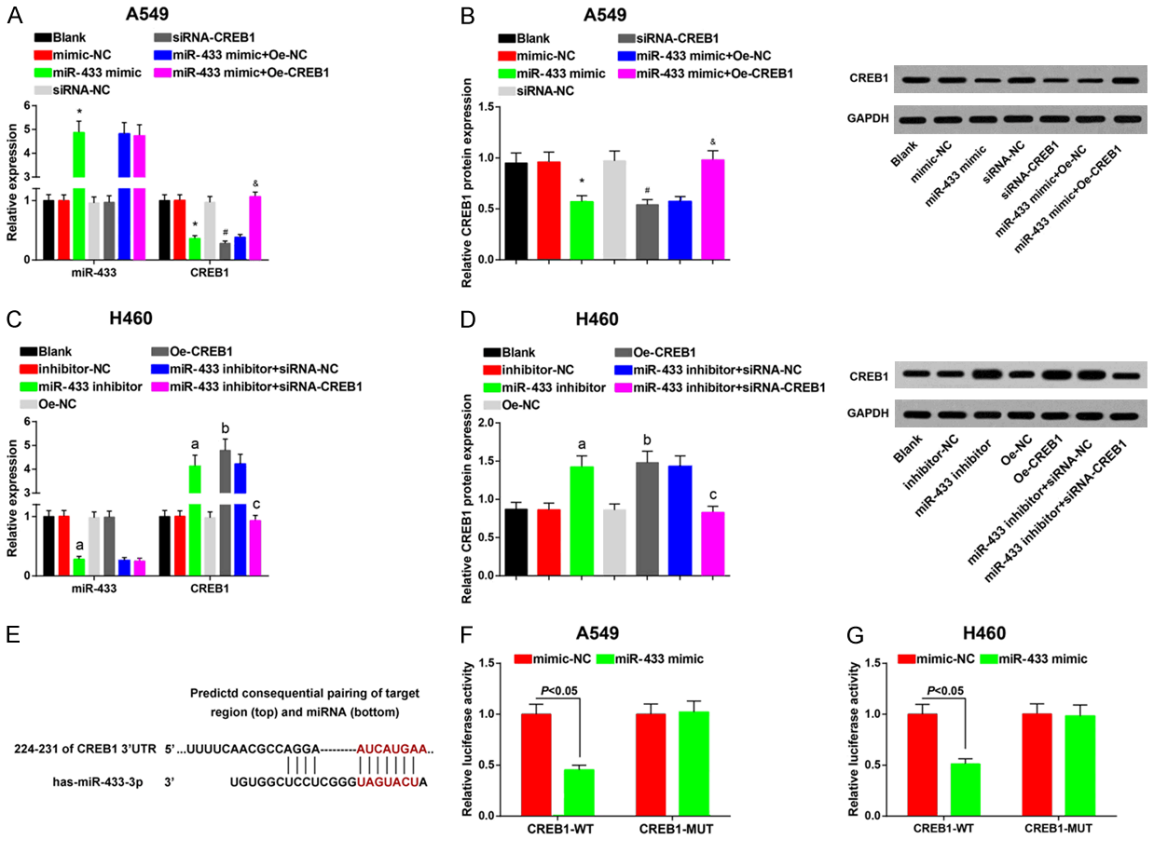

Figure 7. miR-433 targets CREB1. A: miR-433 and CREB1 expressions in the A549 cells of each group using RT-qPCR; B: Western blot analysis verified the CREB1 protein expressions of A549 cells; C: The miR-433 and CREB1 expressions in the H460 cells of each group using RT-qPCR; D: A Western blot analysis verified the CREB1 protein expressions of the H460 cells; E: Prediction of the binding sites between miR-433 and CREB1 using an online website; F, G: Dual luciferase reporter gene assays determined the target relationship between miR-433 and CREB1 in the A549 cells and H460 cells. n = 5 for each group. Compared with the mimic-NC group, *P<0.05. the siRNA-NC group, $^{\#}$P<0.05. Compared with the miR-433 mimic + Oe-NC group, $^{\&}$P<0.05. Compared with the inhibitor-NC group, ^{a}P<0.05. Compared with the Oe-NC group, ^{b}P<0.05. Compared with the miR-433 inhibitor + siRNA-NC group, ^{c}P<0.05. The measurement data are shown as the mean ± standard deviation. The comparisons between two groups were conducted using *t* tests. The comparison among multiple groups were assessed using one-way ANOVA followed by LSD-t tests. CREB1: cyclic-AMP responsive element binding protein 1; miR-433: microRNA-433.

ties of the A549 and H460 cells were similar in the CREB1-MUT and miR-433 mimic groups (both P>0.05) (**Figure 7F** and **7G**), revealing that CREB1 was the direct target gene of miR-433.

Upregulated miR-433 decelerated the A549 xenograft growth while downregulated miR-433 accelerated the H460 xenograft growth

The tumor size was measured every 5 d after the injections of the A549 and H460 cells, and the xenografts were isolated and weighed on the 30th d. It was found that the tumor volumes and weights in the miR-433 mimic group were decreased versus the mimic-NC group. The tumor volumes and weights were increased in the miR-433 inhibitor group more than they were in the inhibitor-NC group (P<0.05) (**Figure 8**).

Discussion

Lung cancer is the main cause of cancer and cancer-related mortality, with about 1.8 million people dying every year [19, 20]. A recent study has suggested that in bladder tumors, c-Met and CREB1 exert a vital function on the inhibition of miR-433-mediated epithelial mesenchymal transition by modulating the Akt/GSK-3β/Snail signaling pathway [21]. Karolina et al. showed that miR-433 overexpression advanc-

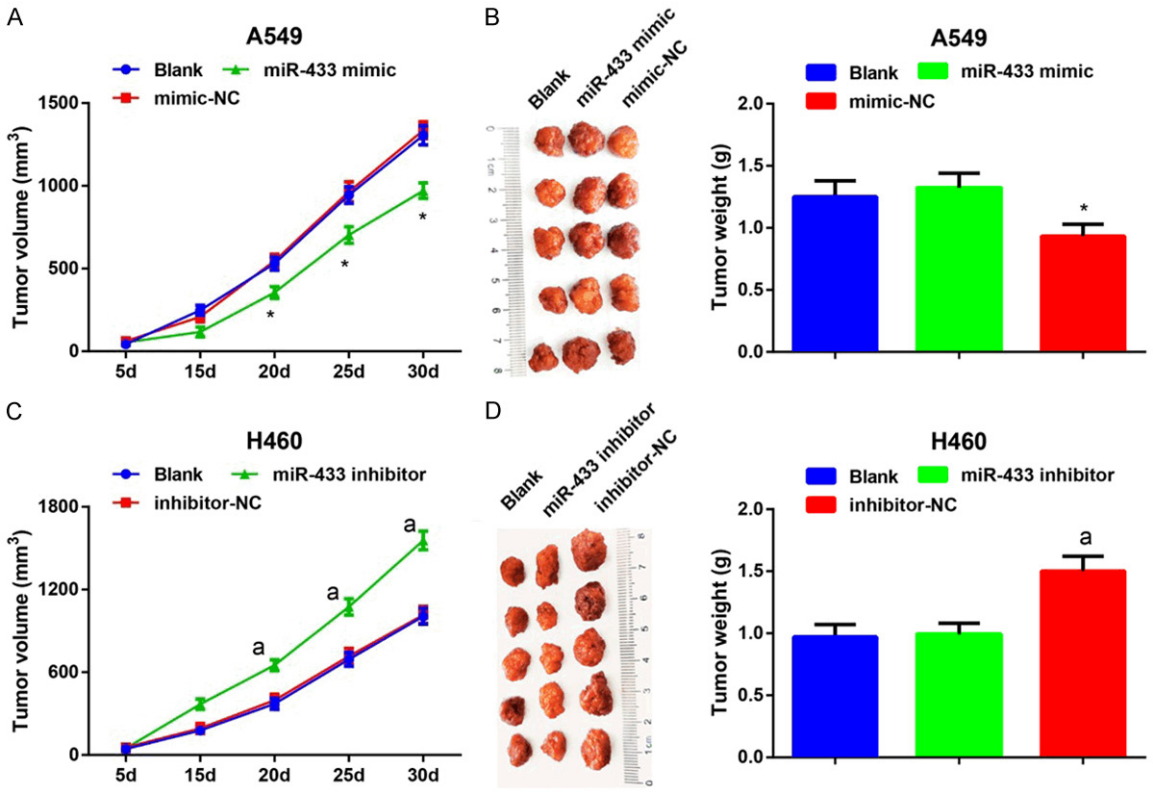

Figure 8. Upregulated miR-433 decelerates A549 xenograft growth while downregulated miR-433 accelerates H460 xenograft growth. A: Changes in the volumes of the A549 xenografts; B: Representative figures for the A549 xenografts and the tumor weights on the 30th d of injection; C: Changes in the volumes of the H460 xenografts; D: Representative figures for the H460 xenografts and the tumor weights on the 30th d of injection. n = 5 mice for each group. Compared with the mimic-NC group, *P<0.05. Compared with the inhibitor-NC group, ^{a}P<0.05. The measurement data are shown as the mean ± standard deviation. The comparison among multiple groups were assessed using one-way ANOVA followed by LSD-t tests. miR-433: microRNA-433.

es paclitaxel resistance by inducing ovarian cancer cell cellular senescence [22]. It is thought that the inhibition of SETD2 or CREB1 produces cisplatin resistance by inhibiting the activation of H3K36me3 and ERK in NSCLC cells [12]. Efforts should be made to deeply understand NSCLC disease. Our investigation showed that miR-433 and CREB1 may be potential candidate markers which could modulate the invasion, migration, proliferation, and the apoptosis of NSCLC cells.

Our study provides substantial evidence that miR-433 expressions are decreased in NSCLC tissues, and the methylating rate is enhanced. A recent study found that in the testing and confirmation of a patient cohort, miR-433 expression in colorectal cancer is downregulated, while the low expression of miR-433 is related to early recurrence and advanced tumor stage [23]. It has been proved that miR-433 is downregulated in retinoblastoma tissues, indicating that miR-433 might be of great importance in retinoblastoma development [24]. It has been reported that in the adjacent normal tissues, miR-433 is often downregulated in oral squamous cell carcinoma, which is in line with our findings. Furthermore, we found that the methylation rate of the CpG island of the miR-433 promoter was increased in the NSCLC tissues when compared to the adjacent normal tissues. Other studies reported that miR-433 is situated in a region rich in CpG in the genomic locus, and the miR-433 expression was modulated by DNA methylation in hepatocellular carcinoma (HCC) cells, which is consistent with our study [17, 25].

In this study, we found that among the five NSCLC cell lines, the A549 cells had the lowest level of miRNA-433 and the highest level of CREB1, while the H460 cells had the highest

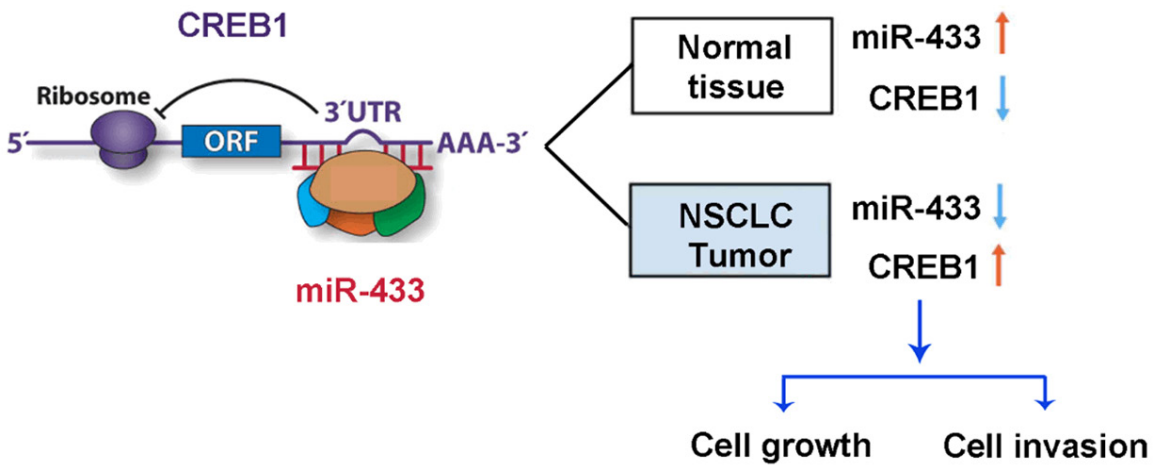

Figure 9. A schematic diagram showing the effects of miR-433 and CREB1 on NSCLC development. CREB1: cyclic-AMP responsive element binding protein 1; miR-433: microRNA-433; NSCLC: non-small cell lung cancer cells.

level of miRNA-433 and the lowest level of CREB1 (**Figure 2A**). Therefore, we treated the A549 cells with an miRNA-433 mimic and/or siRNA-CREB1 and H460 cells with an miRNA-433 inhibitor and/or OE-CREB1 as to verify the effects of miRNA-433 and CREB1 on the lung cancer cell functions. This was consistent with other studies that used two cell lines receiving different treatments [26]. The upregulation of miR-433 or the downregulation of CREB1 suppresses the malignant behaviors of A549 cells. On the other hand, the H460 cells with downregulated miR-433 or upregulated CREB1 showed the opposite results. It has been clarified that upregulated miR-433 suppresses cell viability and proliferation in breast cancer BT-549 cells [27]. It is reported that upregulated miR-433 inhibits the invasion and proliferation of colon cancer cells, while the miR-433 knockout heightens the proliferation and invasion of colon cancer cells [28]. Another study found that upregulated miR-433 can decrease the survival rate of colorectal cancer cells and boost the apoptosis of colorectal cancer cells by downregulating MACC1 [29]. It has been shown that the LILRB2/SHP2/CAMK1/CREB axis is implicated in the migration and proliferation of A549 cells [30]. Another study has also revealed that siRNA against CREB1 suppresses the invasion and migration of HCC MHCC97H cells and antagonizes the role of miR-433. Interestingly, CREB1 siRNA can reduce the proliferation of MHCC97H cells without being affected by the anti-miR-433 [17]. Additionally, in this study, upregulated miR-433 suppressed the CREB1 expressions, and it was further confirmed that CREB1 is a direct target gene of miR-433. Prior research widely confirms that both CREB1 and c-Met are target genes of miR-433 [21]. Moreover, CREB1 is targeted by miR-433 and is able to activate miR-433 expression, thus forming a feedback loop between miR-433 and CREB1 [10]. All this evidence points to the combined effect of miR-433 and CREB1 in NSCLC development.

There are some limitations to this study. Although we verified the effects and relationship of miRNA-433 and CREB1 in the NSCLC cell lines, the miRNA-433 and CREB1-mediated signal pathways related to lung cancer cell growth and metastasis were not validated in this study. This awaits further investigation. Secondly, the combined effects of miRNA-443 and CREB1 on tumor growth in vivo are required to further confirm their relationship in NSCLC development. Last but not least, the correlation between miRNA-433 and the CREB1 expressions in NSCLC patients is needed for further verification using the available online database or an IHC staining analysis.

To briefly conclude, our study offers evidence that DNA methylation can downregulate miR-433 in NSCLC and advance the invasion and proliferation as well as inhibit the apoptosis of NSCLC cells (**Figure 9**). These findings provide a new approach in a novel target therapy for NSCLC. Nevertheless, further efforts are needed to illustrate the potential mechanism.

Disclosure of conflict of interest

None.

Address correspondence to: Xian'en Fa, Department of Cardiac Surgery, The Second Affiliated Hospital of Zhengzhou University, No. 2 Jingba Road, Jinshui District, Zhengzhou 450014, He'nan Province, China. Tel: +86-0371-63934118; Fax: +86-0371-63934118; E-mail: faxianen451@163.com

References

[1] Qu J, Cheng T, Liu L, Heng J, Liu X, Sun Z, Wang W, Li K and Yang N. Mast cells induce epithelial-to-mesenchymal transition and migration in non-small cell lung cancer through IL-8/Wnt/β-catenin pathway. J Cancer 2019; 10: 5567.

[2] Chen W, Zheng R, Baade PD, Zhang S, Zeng H, Bray F, Jemal A, Yu XQ and He J. Cancer statistics in China, 2015. CA Cancer J Clin 2016; 66: 115-132.

[3] Zhao Z, Liu B, Sun J, Lu L, Liu L, Qiu J, Li Q, Yan C, Jiang S, Mohammadtursun N, Ma W, Li M, Dong J and Gong W. Scutellaria flavonoids effectively inhibit the malignant phenotypes of non-small cell lung cancer in an Id1-dependent manner. Int J Biol Sci 2019; 15: 1500-1513.

[4] Shriwash N, Singh P, Arora S, Ali SM, Ali S and Dohare R. Identification of differentially expressed genes in small and non-small cell lung cancer based on meta-analysis of mRNA. Heliyon 2019; 5: e01707.

[5] Ettinger DS, Wood DE, Aisner DL, Akerley W, Bauman J, Chirieac LR, D'Amico TA, DeCamp MM, Dilling TJ, Dobelbower M, Doebele RC, Govindan R, Gubens MA, Hennon M, Horn L, Komaki R, Lackner RP, Lanuti M, Leal TA, Leisch LJ, Lilenbaum R, Lin J, Loo BW Jr, Martins R, Otterson GA, Reckamp K, Riely GJ, Schild SE, Shapiro TA, Stevenson J, Swanson SJ, Tauer K, Yang SC, Gregory K and Hughes M. Non-small cell lung cancer, version 5.2017, NCCN clinical practice guidelines in oncology. J Natl Compr Canc Netw 2017; 15: 504-535.

[6] Li J, Tao X, Shen J, Liu L, Zhao Q, Ma Y, Tao Z, Zhang Y, Ding B and Xiao Z. The molecular landscape of histone lysine methyltransferases and demethylases in non-small cell lung cancer. Int J Med Sci 2019; 16: 922-930.

[7] Pastorkova Z, Skarda J and Andel J. The role of microRNA in metastatic processes of non-small cell lung carcinoma. Biomed Pap Med Fac Univ Palacky Olomouc Czech Repub 2016; 160: 343-357.

[8] Zhou S, Zhang Z, Zheng P, Zhao W and Han N. MicroRNA-1285-5p influences the proliferation and metastasis of non-small-cell lung carcinoma cells via downregulating CDH1 and Smad4. Tumour Biol 2017; 39: 10104283-17705513.

[9] Wang P, Lv HY, Zhou DM and Zhang EN. miR-204 suppresses non-small-cell lung carcinoma (NSCLC) invasion and migration by targeting JAK2. Genet Mol Res 2016; 15.

[10] Yan L, You WQ, Sheng NQ, Gong JF, Hu LD, Tan GW, Chen HQ and Wang ZG. A CREB1/miR-433 reciprocal feedback loop modulates proliferation and metastasis in colorectal cancer. Aging (Albany NY) 2018; 10: 3774-3793.

[11] Liu N, Liu Z, Zhang W, Li Y, Cao J, Yang H and Li X. MicroRNA-433 reduces cell proliferation and invasion in non-small cell lung cancer via directly targeting E2F transcription factor 3. Mol Med Rep 2018; 18: 1155-1164.

[12] Kim IK, McCutcheon JN, Rao G, Liu SV, Pommier Y, Skrzypski M, Zhang YW and Giaccone G. Acquired SETD2 mutation and impaired CREB1 activation confer cisplatin resistance in metastatic non-small cell lung cancer. Oncogene 2019; 38: 180-193.

[13] Li M, Luo XJ, Rietschel M, Lewis CM, Mattheisen M, Müller-Myhsok B, Jamain S, Leboyer M, Landén M, Thompson PM, Cichon S, Nöthen MM, Schulze TG, Sullivan PF, Bergen SE, Donohoe G, Morris DW, Hargreaves A, Gill M, Corvin A, Hultman C, Toga AW, Shi L, Lin Q, Shi H, Gan L, Meyer-Lindenberg A, Czamara D, Henry C, Etain B, Bis JC, Ikram MA, Fornage M, Debette S, Launer LJ, Seshadri S, Erk S, Walter H, Heinz A, Bellivier F, Stein JL, Medland SE, Arias Vasquez A, Hibar DP, Franke B, Martin NG, Wright MJ and Su B. Allelic differences between Europeans and Chinese for CREB1 SNPs and their implications in gene expression regulation, hippocampal structure and function, and bipolar disorder susceptibility. Mol Psychiatry 2014; 19: 452-461.

[14] Wong JC, Bathina M and Fiscus RR. Cyclic GMP/protein kinase G type-Iα (PKG-Iα) signaling pathway promotes CREB phosphorylation and maintains higher c-IAP1, livin, survivin, and Mcl-1 expression and the inhibition of PKG-Iα kinase activity synergizes with cisplatin in non-small cell lung cancer cells. J Cell Biochem 2012; 113: 3587-3598.

[15] Chung JH, Kim DH, Kim YS, Son BS, Kim D, Hwang C, Shin D, Noh SG, Han JH, Kim DK, Kim JH, Koo JS, Chung HY and Yoon SH. Upregulation of P21-activated kinase 1 (PAK1)/CREB axis in squamous non-small cell lung carcinoma. Cell Physiol Biochem 2018; 50: 304-316.

[16] Hu WL and Zhou XH. Identification of prognostic signature in cancer based on DNA methylation interaction network. BMC Med Genomics 2017; 10 Suppl 4: 63.

[17] Yang Z, Tsuchiya H, Zhang Y, Hartnett ME and Wang L. MicroRNA-433 inhibits liver cancer cell migration by repressing the protein expression and function of cAMP response element-binding protein. J Biol Chem 2013; 288: 28893-28899.
[18] You J, Cheng J, Yu B, Duan C and Peng J. Baicalin, a Chinese herbal medicine, inhibits the proliferation and migration of human non-small cell lung carcinoma (NSCLC) Cells, A549 and H1299, by activating the SIRT1/AMPK signaling pathway. Med Sci Monit 2018; 24: 2126-2133.
[19] Chang J, Gao F, Chu H, Lou L, Wang H and Chen Y. miR-363-3p inhibits migration, invasion, and epithelial-mesenchymal transition by targeting NEDD9 and SOX4 in non-small-cell lung cancer. J Cell Physiol 2020; 235: 1808-1820.
[20] Bray F, Ferlay J, Soerjomataram I, Siegel RL, Torre LA and Jemal A. Global cancer statistics 2018: GLOBOCAN estimates of incidence and mortality worldwide for 36 cancers in 185 countries. CA Cancer J Clin 2018; 68: 394-424.
[21] Xu X, Zhu Y, Liang Z, Li S, Xu X, Wang X, Wu J, Hu Z, Meng S, Liu B, Qin J, Xie L and Zheng X. c-Met and CREB1 are involved in miR-433-mediated inhibition of the epithelial-mesenchymal transition in bladder cancer by regulating Akt/GSK-3β/Snail signaling. Cell Death Dis 2016; 7: e2088.
[22] Weiner-Gorzel K, Dempsey E, Milewska M, McGoldrick A, Toh V, Walsh A, Lindsay S, Gubbins L, Cannon A, Sharpe D, O'Sullivan J, Murphy M, Madden SF, Kell M, McCann A and Furlong F. Overexpression of the microRNA miR-433 promotes resistance to paclitaxel through the induction of cellular senescence in ovarian cancer cells. Cancer Med 2015; 4: 745-758.
[23] Zhang J, Zhang L, Zhang T, Dong XM, Zhu Y and Chen LH. Reduced miR-433 expression is associated with advanced stages and early relapse of colorectal cancer and restored miR-433 expression suppresses the migration, invasion and proliferation of tumor cells in vitro and in nude mice. Oncol Lett 2018; 15: 7579-7588.
[24] Li X, Yang L, Shuai T, Piao T and Wang R. MiR-433 inhibits retinoblastoma malignancy by suppressing Notch1 and PAX6 expression. Biomed Pharmacother 2016; 82: 247-255.
[25] Wang XC, Ma Y, Meng PS, Han JL, Yu HY and Bi LJ. miR-433 inhibits oral squamous cell carcinoma (OSCC) cell growth and metastasis by targeting HDAC6. Oral Oncol 2015; 51: 674-682.
[26] Li X, Zhu J, Liu Y, Duan C, Chang R and Zhang C. MicroRNA-331-3p inhibits epithelial-mesenchymal transition by targeting ErbB2 and VAV2 through the Rac1/PAK1/β-catenin axis in non-small-cell lung cancer. Cancer Sci 2019; 110: 1883-1896.
[27] Hu X, Wang J, He W, Zhao P and Ye C. MicroRNA-433 targets AKT3 and inhibits cell proliferation and viability in breast cancer. Oncol Lett 2018; 15: 3998-4004.
[28] Li H, Li J, Yang T, Lin S and Li H. MicroRNA-433 represses proliferation and invasion of colon cancer cells by targeting homeobox A1. Oncol Res 2018; 26: 315-322.
[29] Li J, Mao X, Wang X, Miao G and Li J. miR-433 reduces cell viability and promotes cell apoptosis by regulating MACC1 in colorectal cancer. Oncol Lett 2017; 13: 81-88.
[30] Liu X, Yu X, Xie J, Zhan M, Yu Z, Xie L, Zeng H, Zhang F, Chen G, Yi X and Zheng J. ANGPTL2/LILRB2 signaling promotes the propagation of lung cancer cells. Oncotarget 2015; 6: 21004-21015.